4. Computer modeling of bioimpedance

The object of this chapter is to describe the development and use of a custom developed software package to simulate the electrical impedance of living tissues at the α and β dispersion regions. It is based on the generation of a SPICE netlist from the specification of some numerical parameters concerning the tissue and a bi-dimensional map representing a slice of tissue. Some examples are provided to demonstrate its feasibility.

A significant achievement of *Bioimpedance Simulator* is that it is able to obtain Cole compatible behaviours from models based on simple resistances and capacitances. That is, it shows that the Cole behaviour of living tissues can be related to its structure at cell level and that it is not necessary to consider special electrical properties of cell membranes.

This work is presented in part in:
Ivorra, A., Gómez, R., and Aguiló, J. A SPICE netlist generator to simulate living tissue electrical impedance. 317-320. 2004. Gdansk, Poland. Proceedings of XII International Conference on Electrical BioImpedance (ICEBI). 20-6-2004.

A drawback of electrical bioimpedance measurements is their lack of specificity, that is, different physiological causes can induce the same impedance response and vice versa. Because of that, some authors, including some of the most experienced researchers, just describe the empirical results with some mathematical formulae and do not try to provide any physical interpretation [1]. On the other hand, there are those who prefer to translate the data into equivalent circuit models in order to attribute a physical meaning to the results. Of course, this approach sounds more interesting because it permits a certain correlation between the impedance measurements and some physiological events and, in turn, helps to introduce the bioimpedance methods into the biomedical environments. However, in order to provide any physical interpretation it is first necessary to develop reasonable models able to reproduce the bioimpedance results.

The passive electric properties of biological beings are not constant over the whole frequency spectrum. Some transition regions, known as dispersion regions, can be observed. Schawn [2] defined three frequency regions for the dielectric properties of biological materials: α, β and γ. The large dielectric dispersions appearing between 10 Hz and tens of MHz (α and β dispersion regions) are generally considered to be associated with the diffusion processes of the ionic species (α dispersion) and the dielectric properties of the cell membranes and their interactions with the extra and intracellular electrolytes (β dispersion). The dielectric properties at the γ region (> 100 MHz) are mostly attributed to the aqueous content of the biological species and the presence of small molecules [3]. Additionally, some authors also cite a fourth main dispersion called δ between the β and γ the dispersions, around 100 MHz, [4] that would be caused by the dipolar moments of large molecules such as proteins.

The α and β dispersions are related to the tissular and cellular structures and that makes them specially attractive to detect tissue pathologies such as ischemic injury or tumors.

There exist some attempts to relate the tissue structures with the bioimpedance measurements in the α and β dispersion regions by using analytical models linked with some physical properties of cells and tissues [5]. These analytical models can work properly in some cases such as cell suspensions, however, their applicability is limited when complex structures, such as living tissues, are considered. In those cases, it is advisable to use computer models and simulations if it is not possible to simplify the geometry of the case.

Although not many, there are some examples of computer simulations of electrical bioimpedance at cellular level [6;7]. Most of those simulations are based on Finite Element Analysis (FEA) [8] and that implies the use of software tools that require a high degree of expertise because of its complexity.

Here it is presented the development and use of an alternative method to simulate the electrical impedance of living tissues: the *Bioimpedance Simulator* software package. The *Bioimpedance Simulator* generates SPICE input files, also referred as SPICE netlists, for

simulating the electrical passive properties of living tissues (see Figure 4.1). SPICE stands for "Simulation Program with Integrated Circuit Emphasis" and it was originally conceived more than thirty years ago at the University of California at Berkeley to simulate and predict the behavior of electronic circuits [9]. Now, its successors can be based on different routines but they have inherited the syntax to describe the electronic circuits. The *Bioimpedance Simulator* describes the modeled circuits using that syntax and specifically adjusts it for SPICE OPUS 2.03 (http://fides.fe.uni-lj.si/spice/). Compared with FEA tools the *Bioimpedance Simulator* not only offers simplicity but also provides the SPICE analysis power.

The use of SPICE to simulate the electrical impedance or other electromagnetic properties of living tissues is not a novelty [10;11] but, as far as we know, it has never been used to simulate the impedance of cells or groups of cells with arbitrary shapes . Moreover, up to now, there not exist any publicly available electrical bioimpedance simulator based on this approach.

The *Bioimpedance Simulator* is mainly intended for didactic purposes but it can be also applied to validate some hypothesis concerning the interpretation of the experimental impedance measurements. However, it must be always taken into account that it is a bi-dimensional tool and not all the results can be extrapolated to the three-dimensional problems.

The *Bioimpedance Simulator* including its help documentation and its Visual Basic source files are freely available at http://www.cnm.es/~mtrans/BioZsim/
The software package has been tested on Windows 98 and Windows XP platforms.
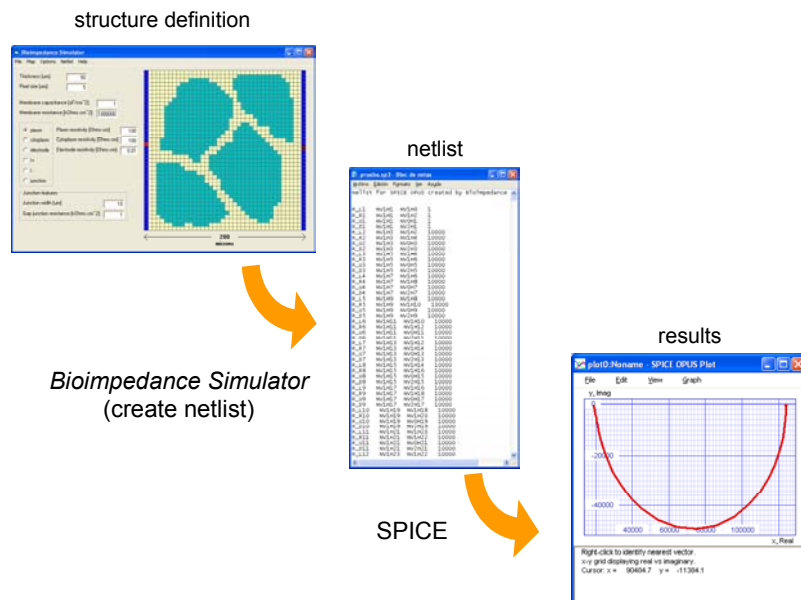

Figure 4.1. Flow diagram representing the use of *Bioimpedance Simulator* to model the electrical bioimpedance of living tissues.

4.1.   Simulator implementation

The *Bioimpedance Simulator* generates a netlist that represents a flat section, or more precisely a slice, of living tissue. Basically, it consists of a bi-dimensional mesh of passive electric components that depend on some numerical parameters, such as the plasm and cytoplasm resistivities, and a bi-dimensional map drawn by the user. Each square pixel of the map is transformed into a set of passive circuit components (resistances and capacitances) interconnected between them and the components of the adjacent pixels. The type of components, their interconnections, and their values depend on the elements (colors) drawn by the user. Table 4.1. summarizes those elements and their modeling. Figure 4.2 depicts a map example including all the elements that can be modeled. Note that the *Bioimpedance Simulator* generates a netlist to simulate two-electrode impedance measurements, however, it is possible to edit those netlist files to create the analysis for other kinds of measurement (e.g. four-electrode measurements).
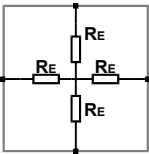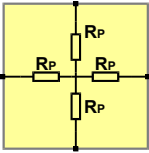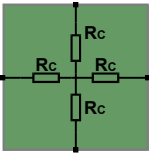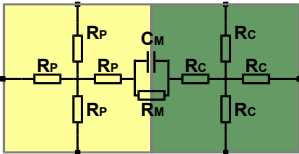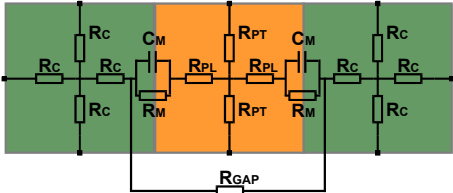
The electrode, plasm (extra-cellular medium) and cytoplasm elements are modeled as pure resistive media. At any plasm-cytoplasm interface the presence of the cell membrane is assumed and it is modeled as a capacitance in parallel with a resistance. The resistive behavior of plasm and cytoplasm and the dielectric behavior of cell membrane is a commonly accepted simplification by most researchers [12], at least up to some MHz.

At the tight inter-cell spaces it is possible to find special structures (gap junctions) that allow ions to flow from the cytoplasm of one cell to the cytoplasm of the adjacent cell. These behavior is modeled by the *Bioimpedance Simulator* as shunting resistances (R_{GAP}).
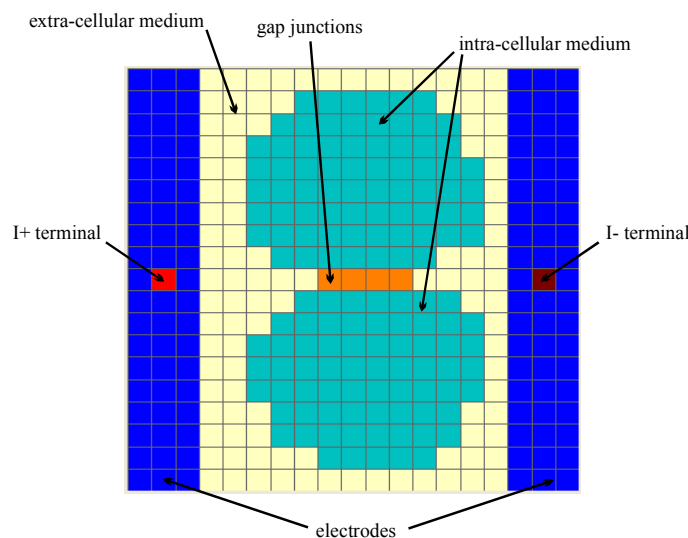
Figure 4.2. All the elements that can be simulated by the *Bioimpedance Simulator* are depicted in this figure. Two cells inter-connected through gap junctions are measured by means of two electrodes. The generated netlist specifies that the impedance is measured between the central nodes of two pixels (I+ terminal and I- terminal).

Table 4.1. Bioimpedance Simulator elements and their equivalent circuits.

Element	Equivalent circuit	Equations	Notes
electrode		$R_E = \dfrac{\rho_E / 2}{T}$	ρ_E = electrode material resistivity T = slab thickness
plasm		$R_P = \dfrac{\rho_P / 2}{T}$	ρ_P = plasm resistivity
cytoplasm		$R_C = \dfrac{\rho_C / 2}{T}$	ρ_C = cytoplasm resistivity
cell membrane		$C_{CM} = c_M \cdot PS \cdot T$ $R_M = \dfrac{r_M}{PS \cdot T}$	c_M = unitary membrane capacitance r_M = unitary membrane resistance PS = pixel size
gap junctions		$R_{GAP} = \dfrac{r_G}{PS \cdot T}$ $R_{PL} = \dfrac{\rho_P (JW/2)}{PS \cdot T}$ $R_{PT} = \dfrac{\rho_P (PS/2)}{JW \cdot T}$	r_G = unitary junction resistance JW = junction width

4.2.   Results

The *Bioimpedance Simulator* was satisfactorily tested by simulating well known structures such as tracks, corners, parallel plates and strip lines. In this section, the

simulations of other structures related with the bioimpedance field are presented as examples to show the applicability of the simulator.

## 4.2.1. Cell suspension conductivity

From the electrical point of view, one of the simplest physical models for biological samples is a suspension of spherical particles in an electrolytic solution. Such a model is not suitable for most living tissues but it has proven to be effective in the case of dilute blood or cell suspensions. Some expressions have been analytically derived according to this model. The Maxwell-Fricke equation (equation 4.1) is one of these analytical solutions [12].

By using the *Bioimpedance Simulator*, the low frequency conductivity of a cell suspension was simulated and compared to that expected from the Maxwell-Fricke equation:

$$\frac{(\sigma - \sigma_a)}{(\sigma + \gamma\sigma_a)} = p\frac{(\sigma_i - \sigma_a)}{(\sigma_i + \gamma\sigma_a)} \tag{4.1}$$

where σ is the conductivity of the total suspension, σ_a is the plasm conductivity, σ_i is the cytoplasm conductivity (since cells are completely isolated at low frequencies $\sigma_i = 0$ Ω/cm), p is the cells volume fraction and γ is a shape factor that is equal to 1 for cylinders normal to the electrical field as it is the case for the *Bioimpedance Simulator*.

Figure 4.3 shows the results from that comparison in the case that cylindrical cells with radius equal to 4.5 squares are studied in a 40×40 square map. Note that, although the resolution is too low to properly draw the circumferences, the *Bioimpedance Simulator* results are quite similar to those predicted by the analytical model.
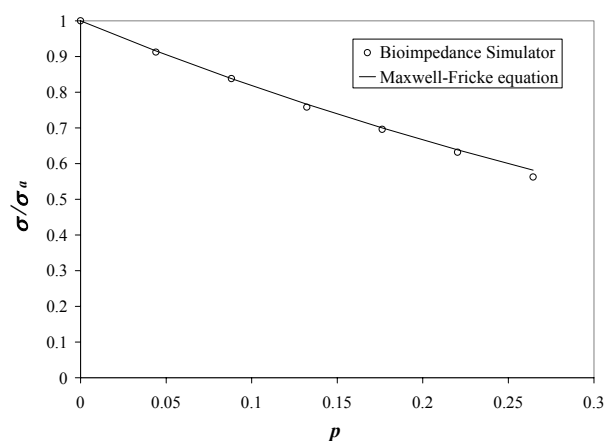

Figure 4.3. Low frequency (<10 Hz) conductivity against cells volume fraction obtained with the *Bioimpedance Simulator* and the analytical model (Maxwell-Fricke equation) (map size= 40×40 squares, cell radius= 4.5 squares, slice thickness=100 μm, pixel size = 10 μm, membrane capacitance = 1 μF/cm², plasm resistivity = cytoplasm resistivity= 100 Ω.cm)

4.2.2.   Gap junctions

As it has been mentioned in section 1.3, the gap junctions are intercellular pores that allow ions and small molecules to flow from the cytoplasm of one cell to the cytoplasm of the adjacent cell. Of course, they are relevant from the electrical bioimpedance point of view and for that reason its behavior can be also modeled by the *Bioimpedance Simulator*.

There are strong evidences that the closure of gap junctions plays an important role in the evolution of impedance during the ischemia events [13-16]. In addition, it has been suggested that the gap junctions are the cause of the low frequency dispersions observed in some normoxic tissues such as the myocardium. The simulation shown in Figure 4.4 reinforces that hypothesis. The structure vaguely resembling the myocardial tissue produces two dispersions: a high frequency dispersion (central frequency ~ 40 kHz) related with the cells and a low frequency dispersion (central frequency ~ 1 kHz) related with the cells grouping caused by the gap junctions. That is, the gap junctions group the cells into larger structures that induce relaxation processes at lower frequencies than the single cells.
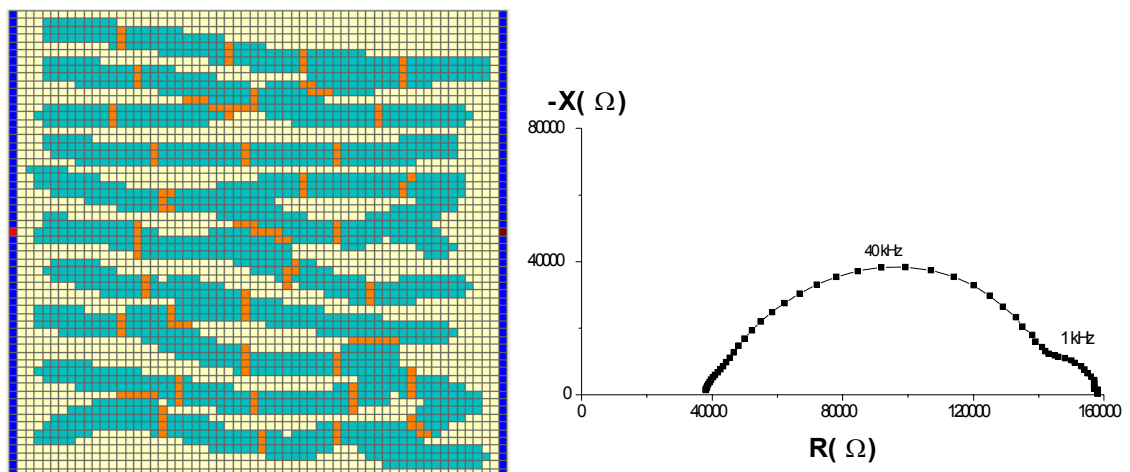

Figure 4.4. (left) Simulated structure resembling a piece of myocardium. The myocardial cells (myocytes) are interconnected through gap junctions. (60 x 60 squares, slice thickness = 25 μm, pixel size = 6 μm, membrane capacitance = 1 μF/cm², plasm resistivity = cytoplasm resistivity = 100 Ω.cm, electrode resistivity = 0.001 Ω.cm, gap junction resistance = 5 Ω.cm², junction width =1 mm). (right) The Nyquist plot shows two dispersions.

4.2.3.   Cell with organelles

The presence of organelles inside the cells has been noted as the cause of the observed secondary dispersions at higher frequencies than the main β dispersion [3]. Aside from the nucleus, the mitochondria could play a significant role in this sense [5;17].

The example shown in Figure 4.5 shows that the presence of organelles can indeed produce such high frequency dispersions (Figure 4.6). Observe that those organelles have been modeled as plasm vesicles inside the cell and that theirs dimensions are comparable to the mitochondria sizes.
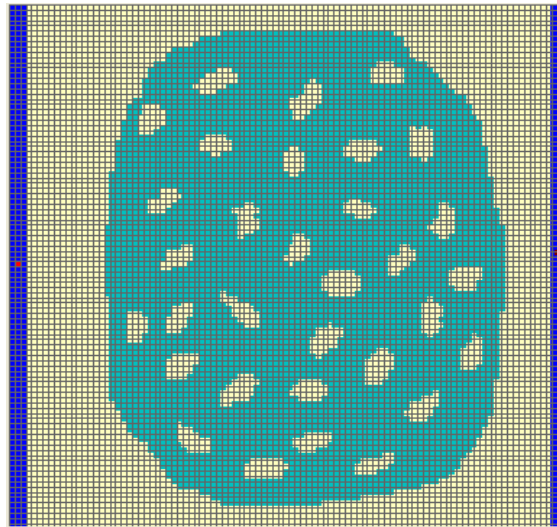
Figure 4.5. Simulated cell containing organelles (100 x 100 squares, slice thickness = 1 μm, pixel size = 0.3 μm, membrane capacitance = 1 μF/cm², plasm resistivity = cytoplasm resistivity = internal organelle resistivity = 100 Ω.cm, electrode resistivity = 0.001 Ω.cm).
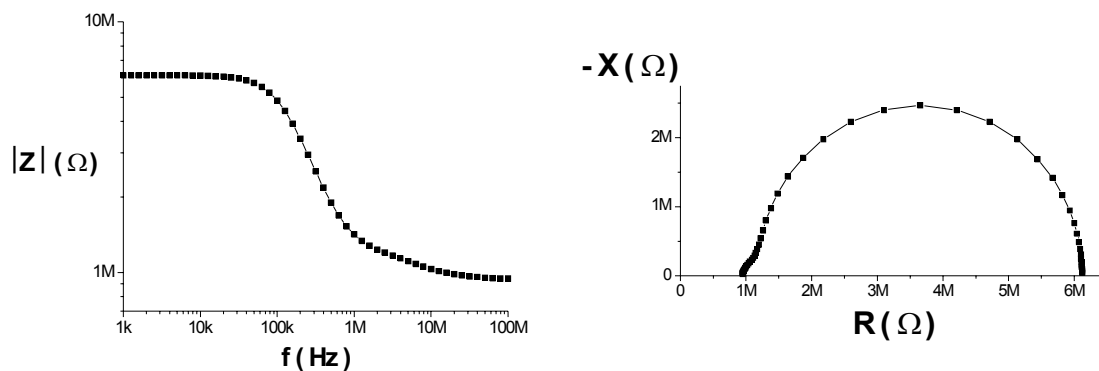

Figure 4.6. (left) Impedance magnitude Bode plot and (right) impedance locus. Both plots show the presence of a dispersion between 1 MHz and 10 MHz that does not appear in the case that the organelles are removed.

4.2.4. Tissue ischemia

One of the most accepted explanations to the fact that tissue bioimpedance magnitude at low frequencies increases during ischemia is the fact that the cell edema, induced by the lack of oxygen, constrains the extracellular space and, consequently, narrows the low frequency current path (see section 1.1.).

The maps depicted in Figure 4.7 were drawn by Luis G. Vázquez de Lara (Benemérita Universidad Autónoma de Puebla) and Luis H. Medina (Universidad Popular Autónoma de Puebla, Puebla, México) to simulate the effect of brain tissue edema caused by ischemia on bioimpedance [18-20].
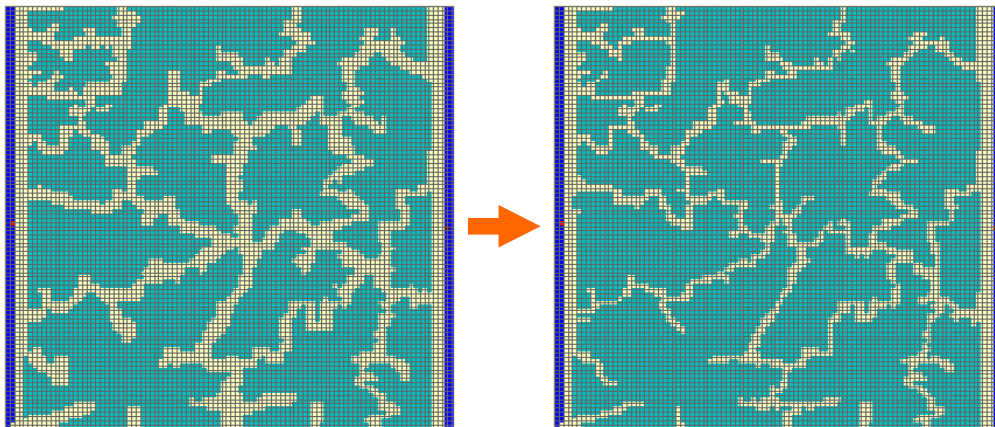
Figure 4.7. (left) Simulated normoxic brain tissue slice and (right) simulated ischemic brain tissue slice (100 x 100 squares, slice thickness = 50 μm, pixel size = 5 μm, membrane capacitance = 1 μF/cm², plasm resistivity = cytoplasm resistivity = internal organelle resistivity = 100 Ω.cm, electrode resistivity = 0.001 Ω.cm).

The simulations results (Figure 4.8) show a significant impedance magnitude increase at low frequencies and a significant phase decrease at low and intermediate frequencies (from 100 Hz to 100 kHz).
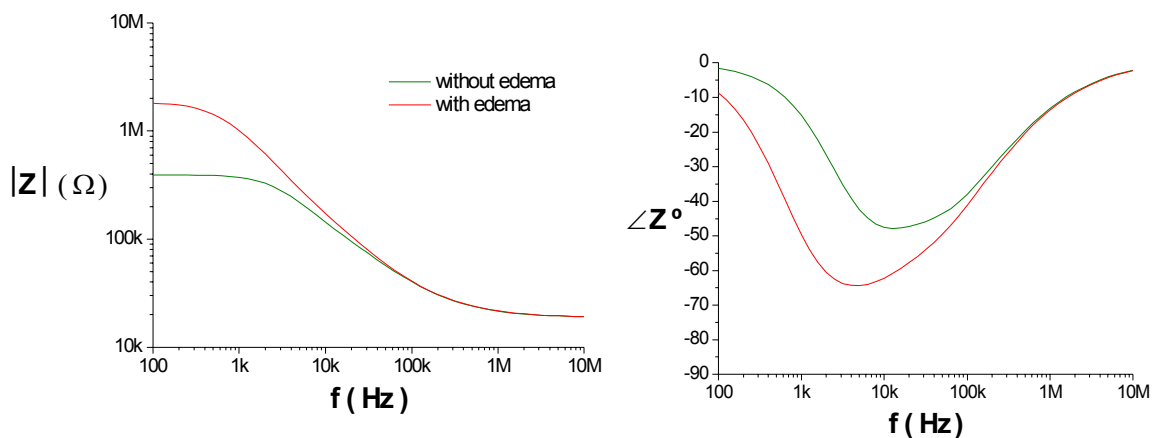

Figure 4.8. Impedance magnitude and phase angle Bode plots obtained from the simulations depicted in Figure 4.7.

4.2.5. Cole bioimpedance model

In 1940 Keneth S.Cole [21] introduced the first mathematical expression able to describe the 'depressed semicircles'[1] found experimentally when measuring living tissues electrical impedance. It is known as the Cole equation (here expressed as in [12]):

$$\mathbf{Z} = R_{\infty} + \frac{\Delta R}{1 + (j\omega\tau)^{\alpha}} \quad , \qquad \Delta R = R_0 - R_{\infty} \tag{4.2}$$

where $\mathbf{Z}$ is the impedance value at frequency ω, j is the complex number $(-1)^{1/2}$, R_{∞} is the impedance at infinite frequency, R_0 is the impedance at zero frequency, τ is the characteristic time constant and α is a dimensionless parameter with a value between 0 and 1. The α parameter is generally around 0.8 for the case of living tissues and it denotes the divergence from the Debye type relaxation[2] ($\alpha = 1$). Its physical meaning is not clearly understood. Some researchers suggest that it is caused by a random distribution of relaxation times due to the heterogeneity of cell sizes and shapes [3]. However, several tries were performed with the *Bioimpedance Simulator* to produce the Cole responses by randomizing cells sizes and shapes and, the only successful results were obtained when unrealistic large differences in cell sizes were introduced. On the other hand, realistic structures such as that shown in Figure 4.9 produced Cole compatible responses. From that kind of simulations it was concluded that the extracellular space morphology is a key factor concerning the α value: the more tortuous it is, the lower α value is obtained.
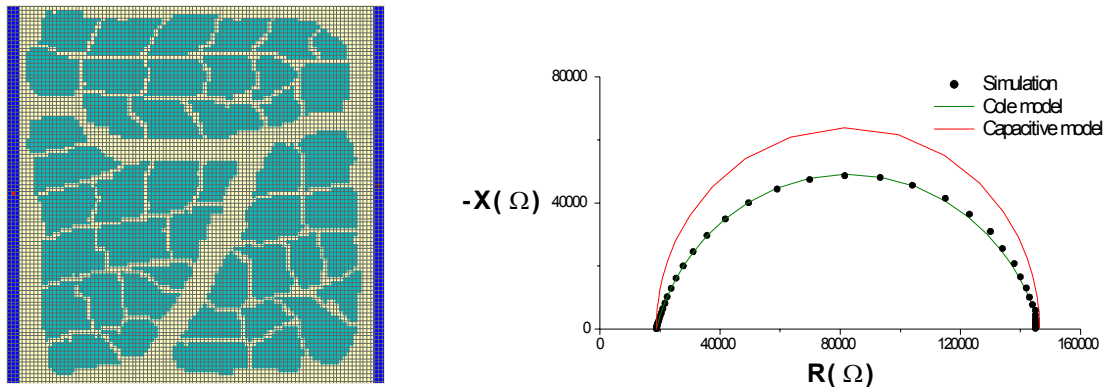
Figure 4.9. (left) Simulated structure resembling an actual tissue cut. It represents three cell clusters separated by large extracellular spaces (vessels). (100×100 squares, slice thickness=50 μm, pixel size = 2 μm, membrane capacitance = 1 μF/cm^{2}, plasm resistivity = cytoplasm resistivity = 100 Ω.cm, electrode resistivity = 0.001 Ω.cm). (right) The results not only differ from the capacitive behavior (Debye type relaxation) but also match the Cole response. By using a commercial software (ZView, Scribner Associates, Inc) the following values are obtained for the Cole equation (4.2): R = 18.7 kΩ, ΔR = 127.6 kΩ, α = 0.835 and τ = 2.88 μs.

---

[1] Cole model and other electrical bioimpedance models are explained in more detail in chapter 5.

[2] The Debye type elaxation corresponds to the simple resistance-capacitance pair.

4.2.6. Solid electrode-electrolyte interface impedance

As it has been mentioned in chapter 2, at the interface between a blocking electrode and an electrolyte, the charge distribution creates what is usually referred as the electrical 'double layer' [22]. The impedance of this double layer is usually represented by a capacitance and, indeed, this ideal behaviour has been observed with liquid mercury electrode systems, which have perfectly smooth surfaces [23]. However, in the case of solid metal electrodes, it has been observed that the impedance of that interface over a wide range of frequencies is more properly modelled by a 'constant phase element' (CPE) whose impedance is:

$$Z = K(j\omega)^{-\beta} \tag{4.2}$$

$$\phi = -\beta(\pi/2) \tag{4.3}$$

The impedance locus (Nyquist plot) of a CPE is a straight line at an angle of ϕ to the real axis which differs from the capacitance model ($\phi = -\pi/2$)

Since there exist many empirical and analytical evidences that the CPE behavior is related with the electrode surface roughness [24] and even with its fractal dimensions [25;26], this phenomenon can be employed to construct an example in order to demonstrate the extended applicability of the *Bioimpedance Simulator*.

Figure 4.10 shows the simulated structure that represents a rough electrode-electrolyte interface with some degree of fractal features. Note that the electrode-electrolyte double layer capacitance was modeled by the cell membrane capacitance (plasm-cytoplasm interface)[3].

As it can be observed, the *Bioimpedance Simulator* results indeed show the CPE behavior ($\phi = -\pi/4$) at high frequencies (>100 Hz).

---

[3] The current version of *Bioimpedance Simulator* does not model at all the electrode-electrolyte interface impedance. That is, the interface between the electrode pixels and the other pixels is modeled as a resistance. Thus, in order to model the actual electrode-electrolyte interface impedance, the electrode was drawn as it was the cytoplasm medium with high conductivity.
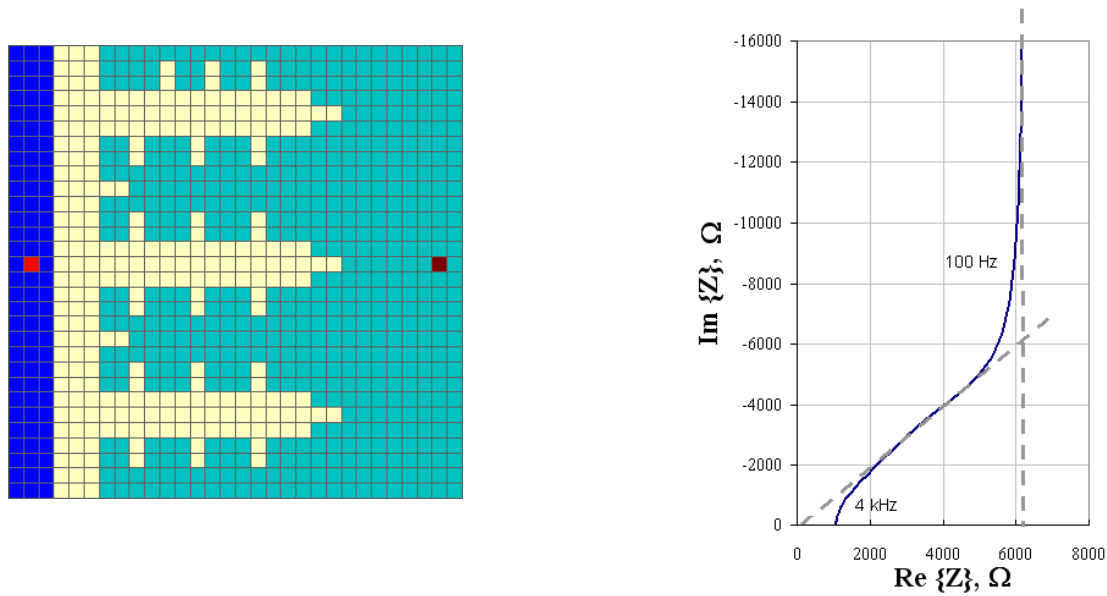
Figure 4.10. (left) Structure to simulate the behaviour of a rough solid electrode-electrolyte interface (slice thickness=100 μm, pixel size = 10 μm, membrane capacitance = 100 μF/cm², plasm resistivity = 100 Ω.cm, cytoplasm resistivity = electrode resistivity = 0.001 Ω.cm). (right) Nyquist plot of the simulated electrode-electrolyte impedance.

References

1. McAdams, E. T., Jossinet, J., and Lackermeier, A., "Modelling the 'Constant Phase Angle' behaviour of biological tissues: potential pitfalls," *Innov.Tech.Biol.Med.*, vol. 16, no. 6, pp. 662-670, 1995.

2. Schwan, H. P., "Electrical properties of tissue and cell suspensions," in Lawrence, J. H. and Tobias, C. A. (eds.) *Advances in Biological and Medical Physics* New York: Academic Press, 1957.

3. Foster, K. R. and Schwan, H. P., "Dielectric properties of tissues and biological materials: a critical review," *CRC Critical Reviews in Biomedical Engineering*, vol. 17 pp. 25-104, 1989.

4. Pethig, R., "Dielectric Properties of Biological Materials: Biophysical and Medical Applications," *IEEE Transactios on Electrical Insulation*, vol. EI-19, no. 5, pp. 453-474, 1984.

5. Raicu, V., Saibara, T., Enzan, H., and Irimajiri, A., "Dielectric properties of rat liver in vivo: analysis by modeling hepatocytes in the tissue architecture," *Bioelectrochemistry and Bioenergetics*, vol. 47 pp. 333-342, 1998.

6. Jones, D. M., Smallwood, R. H., Hose, D. R., Brown, B. H., and Walker, D. C., "Modelling of epithelial tissue impedance measured three different designs of probe," *Physiological Measurement*, vol. 24 pp. 605-623, 2003.

7. Walker, D. C., Brown, B. H., Hose, D. R., and Smallwood, R. H., "Modelling the electrical impedivity of normal and premalignant cervical tissue," *Electronics Letters*, vol. 36, no. 19, pp. 1603-1604, 2000.

8. Miller, C. E. and Henriquez, C. S., "Finite Element Analysis of Bioelectric Phenomena," *Critical Reviews in Biomedical Engineering*, vol. 18 pp. 207-233, 1990.

9. Al-Hashimi, B., *The art of simulation using PSpice: analog and digital* Boca Rato, Florida: CRC Press, 1995.

10. Sperelakis, N. and Sfyris, G., "Impedance Analysis Applicable to Cardiac Muscle and Smooth Muscle Bundles," *IEEE Transactions on Biomedical Engineering*, vol. 38, no. 10, pp. 1010-1022, 1991.

11. Eberdt, M., Brown, P. K., and Lazzi, G., "Two-Dimensional SPICE-Linked Multiresolution Impedance Method for Low-Frequency Electromagnetic Interactions," *IEEE Transactions on Biomedical Engineering*, vol. 50, no. 7, pp. 881-889, 2003.

12. Grimnes, S. and Martinsen, Ø. G., *Bioimpedance and bioelectricity basics* London: Academic Press, 2000.

13. Kléber, A. G., Riegger, C. B., and Janse, M. J., "Electrical uncoupling and increase of extracellular resistance after induction of ischemia in isolated, arterially perfussed rabbit papillary muscle," *Circulation Research*, vol. 61, no. 2, pp. 271-279, 1987.

14. Gersing, E., Hofmann, B., Kehrer, G., and Pottel, R., "Modelling based on tissue structure: the example of porcine liver," *Innov.Tech.Biol.Med.*, vol. 16, no. 6, pp. 671-678, 1995.

15. Groot, J R de, "Genesis of life-threatening ventricular arrhythmias during the delayed phase of acute myocardial ischemia. Role of cellular electrical coupling and myocardial heterogeneities." PhD Thesis University of Amsterdam, 2001.

16. Schaefer, M., Knapp, J., Gross, W., Preuss, M., and Gebhard, M. M. Measurement of electrical cell uncoupling in ischemic mouse heart. 95-98. 2004. Gdansk, Poland. Procedings from the XII International Conference on Electrical BioImpedance (ICEBI). 20-6-0004.
Ref Type: Conference Proceeding

17. Asami, K., Yonezawa, T., Wakamatsu, H., and Koyanagi, N., "Dielectric spectroscopy of biological cells," *Bioelectrochemistry and Bioenergetics*, vol. 40 pp. 141-145, 1996.

18. Demirci, M., Ayata, C., Dalkara, T., Erdemli, G., and Onur, R., "Monitoring cellular edema at single-neuron level by electrical resistance measurements," *Journal of Neuroscience Methods*, vol. 72 pp. 175-181, 1997.

19. Werth, J. L., Park, T. S., Silbergeld, D. L., and Rothman, S. M., "Excitotoxic swelling occurs in oxygen and glucose deprived human cortical slices," *Brain Research*, vol. 782 pp. 248-254, 1998.

20. Lingwood, B. E., Dunster, K. R., Healy, G. N., Ward, L. C., and Colditz, P. B., "Cerebral impedance and neurological outcome following a mild or severe hypoxic/ischemic episode in neonatal piglets," *Brain Research*, vol. 969 pp. 160-167, 2003.

21. Cole, K. S. Permiability and impermiability of cell membranes for ions. 8, 110-122. 1940. Cold Spring. Sympos Quant Biol.
Ref Type: Conference Proceeding

22. Madou, M. J. and Morrison, S. R., "Solid/Liquid Interfaces," *Chemical Sensing with Solid State Devices* Boston: Academic Press, 1989, pp. 105-158.

23. McAdams, E. T., "Effect of surface topography on the electrode-electrolyte interface impedance, 1. The High Frequency (f>1 Hz), Small Signal, Interface Impedance - A Review," *Surface Topography*, vol. 2 pp. 107-122, 1989.

24. De Levie, R., "The influence of surface roughness of solid electrodes on electrochemical measurements," *Electrochimica Acta*, vol. 10 pp. 113-130, 1965.

25. Nyikos, L. and Pajkossy, T., "Fractal dimension and fractional power frequency-dependent impedance of blocking electrodes," *Electrochimica Acta*, vol. 30, no. 11, pp. 1533-1540, 1985.

26. Liu, S. H., "Fractal Model for the ac Response of a Rough Interface," *Physical Review Letters*, vol. 55, no. 5, pp. 529-532, July1985.